Turkish Journal of Electromechanics and Energy
ISSN: 2547-975X
Vol:8, No3, Page 90-96 (2023)
https://www.scienceliterature.com

Turkish Journal of Electromechanics & Energy
an international open access journal

Transforming scrap inner tube rubber into a triboelectric energy harvester

Galip Yılmaz*

Department of Electronics and Automation, Bayburt University, Bayburt, Türkiye

ARTICLE INFO

***Article Type*:**
Research Article

Article History:
Received: 13 October 2023
Revised: 18 November 2023
Accepted: 2 December 2023
Published: 30 December 2023

Editor of the Article:
M. E Şahin

Keywords:
TENG, Upcycling, Inner tube rubber, Energy harvesting, Surface morphology

ABSTRACT

In today's world, the issues of energy shortages, global warming, and pollution caused by reliance on fossil fuels necessitate a swift shift to cleaner energy sources. Triboelectric nano generators (TENGs) present a good remedy for transforming mechanical energy into electricity. This research centres on transforming cast-off inner tube rubber into a TENG that can collect energy from human motion. In this study, surface roughness was improved by sanding, and cost-effective, easily producible TENGs were created using readily available materials such as room-temperature-vulcanizing silicone (RTV silicone). Key findings reveal that inner tube rubber can successfully be upcycled into high-performing TENGs, with sample S2 being particularly noteworthy for generating over 6 Volts and powering four light-emitting diodes (LEDs). Various resistance experiments highlighted the robust energy production potential of these TENGs. Real-world testing of a sports shoe has revealed that the S2 sample can generate more than 15 V, demonstrating the viability of repurposing waste materials for effective energy harvesting.

Cite this article: G. Yılmaz, "Transforming scrap inner tube rubber into a triboelectric energy harvester," Turkish Journal of Electromechanics & Energy, 8(3), pp.90-96, 2023.

1. INTRODUCTION

In today's world, important challenges, including energy shortages, global warming, and pollution, are derived from the significant dependence on fossil fuels [1]. To guarantee the sustainability of our civilization, we must urgently look for cleaner energy sources that do not harm the environment [2–5]. Global warming and energy shortages are major issues requiring research into cleaner energy use. The more energy is consumed, particularly from sources such as oil and coal, the more these problems are exacerbated. Therefore, the fast shift towards cleaner energy sources is critical [6–9].

Efforts to optimize global energy use are increasingly focused on harnessing the abundant clean energy sources available in mechanical motion, such as water waves, wind, raindrops, and biomechanical motion [10–12]. Additionally, the rise of the Internet of Things (IoT) has opened up the potential for this ubiquitous energy emission to power sensors distributed worldwide. Also, rapid advances in personal electronics and sensor networks have increased the demand for portable and sustainable power sources, currently dominated by batteries [13-21].

Triboelectric generators, which have increased rapidly in recent years, have become one of the most emerging tools in converting these existing energy sources into electrical energy. The operation of triboelectric nano generators (TENGs) is based on a combination of contact electrification and electrostatic induction, where the energy conversion efficiency depends on the electrification, which is influenced by the electronegativity of the materials involved [22–24]. Unlike state-of-the-art mechanisms for vibration energy harvesting, which often face limitations like structural complexity, material quality, and external power dependence, TENG stands out for its cost-effectiveness, high energy generation, and ease of production. TENGs have remarkable properties and impressive charge density, making them a versatile and environmentally friendly choice for harvesting mechanical energy, particularly from human motion [16, 23–25].

In the face of the global waste crisis caused by the destruction of plastic and tires, the need for pioneering solutions such as recycling becomes evident. Although plastics have revolutionized modern life, they are also a driver of environmental pollution due to their inherently non-degradable nature. In this context, recycling is a progressive way to renew the economic value of plastics. Various methodologies can transform waste materials into high-performance substances and specialized polymers, thus giving new life to discarded resources [26–30].

Using scrap inner tube rubber as a material for the TENG is significant for sustainable energy harvesting. By transforming discarded inner tube rubber, typically viewed as waste, into a functional component of TENG devices, the research can generate a cost-effective and environmentally friendly route to materials for energy harvesting. The inner tube rubber is one of the products that has reached the end of its lifespan and is accumulating as scrap with each passing day. For example, the

*Corresponding author's e-mail: galipyilmaz@bayburt.edu.tr

inner tubes of farm vehicle tires are becoming gradually obsolete with each passing day of maintenance. Farmers are increasingly choosing to discard these inner tubes rather than repair them. Many of them are increasingly inclined to choose tubeless tires for their convenience and superior performance.

It's worth emphasizing that the exact composition of an inner tube may differ among manufacturers and product lines. Manufacturers often consider the exact blend of rubber compounds and additives proprietary information. In general, the chemical composition of an inner tube consists of synthetic rubber compounds, typically derived from a combination of synthetic elastomers, reinforcing materials, curing agents, and various additives. The specific composition can vary depending on the manufacturer and inner tube type. Common synthetic rubber compounds in inner tubes include butyl rubber, known for its excellent air retention properties and impermeability to gases such as air. It is ideal for maintaining tire pressure. Natural rubber is sometimes used with butyl rubber, providing elasticity and flexibility to the tube. Styrene-butadiene rubber (SBR) is another synthetic option, prized for its abrasion resistance and durability. Vulcanization agents, such as sulfur, are commonly used to strengthen and stabilize the rubber through cross-linking polymer chains. Carbon black serves as a reinforcing filler, enhancing strength, wear resistance, and overall durability. Antioxidants and antiozonants protect the rubber from oxygen and ozone degradation, extending the inner tube's lifespan [31–34]. Using scrap inner tube rubber as a material for the TENG is significant for sustainable energy harvesting. By transforming discarded inner tube rubber, typically viewed as waste, into a functional component of TENG devices, the research can generate a cost-effective and environmentally friendly route to materials for energy harvesting. In the literature reviewed, no publication included upcycling the inner tube as TENG. Experimental studies are needed due to the dynamic and complex structure of the inner tube material to be a TENG device.

This study focuses on upcycling discarded inner tube rubber into a triboelectric nanogenerator technology capable of harvesting energy from human movement on walking and running tracks. The method used aims to be low-cost, easy to control, and easy to apply. Therefore, the surface roughness was increased using a grinding method suitable for mass production to increase the energy harvesting potential. The readily available room-temperature-vulcanizing silicone (RTV silicone) was chosen as the counter material. Similarly, an attempt was made to increase the surface roughness of the RTV. This demonstrated the potential of a discarded product to serve a technological purpose.

2. METHOD

2.1. Preparation of Samples from Inner Tube Material

A sample was prepared from the inner tube material of a tractor's rear wheel that had reached the end of its service life. The interior of the inner tube generally receives talc or a comparable powder treatment to prevent adhering. The trimmed segment was cleansed using soapy water to eliminate residual oil and dust. Figure 1 shows the inner tube material after the cleaning process. This material was measured at a minimum of 10 different points with a micrometre, with an average thickness of 1.50 ± 0.26 mm determined. After cleaning, as shown in Figure 1(b), the samples were cut into 2.5 cm square pieces, attached to a sample holder with double-sided tape, and subjected to sanding. As shown in Figure 1(c), a surface treatment method was applied with sandpapers having grit sizes of P800 (21.8 μm), P1200 (15.3 μm), and P2500 (8 μm). Additionally, one type of sample was set aside for experiments without undergoing any sanding. The prepared samples were then cut to 10 x 10 mm dimensions before being placed into the TENG device and tested.

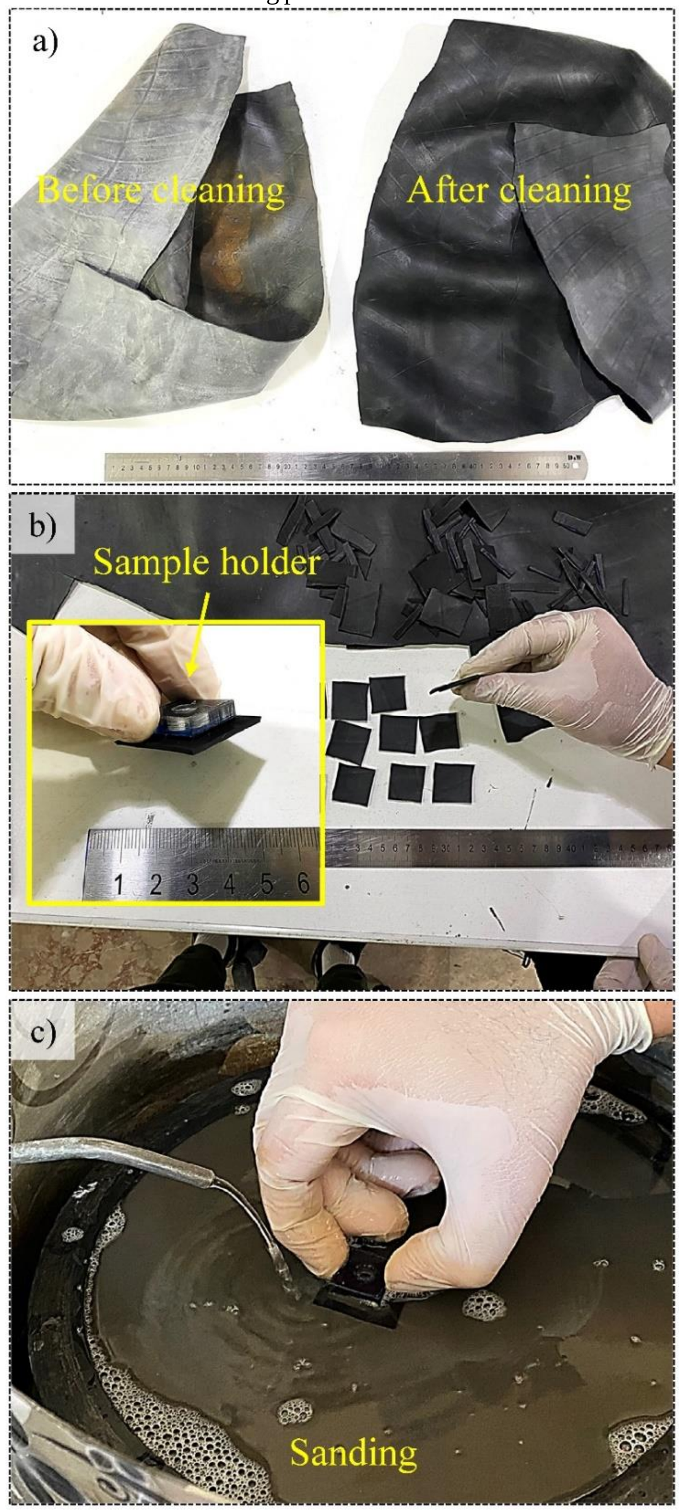

Fig. 1. Sample preparation, (a) Tube material before and after cleaning, (b) cutting and holder, and (c) sanding step of samples on a metallographic grinding machine.

2.2. Preparation of RTV-2 Silicone samples

After trial-and-error experiments, it was decided to use an RTV-2 material as an electron acceptor. RTV material was chosen as the electron acceptor due to its favorable triboelectric properties, compatibility with the replication of surface patterns, and its overall suitability for the fabrication process in the context of the TENG device. RTV-2 is room-temperature curing silicone materials that consist of two components: one containing a cross-linking agent or catalyst and the other the resin-based part. When these two components are mixed, they react to produce the desired properties. These RTV-2 silicones can be customized to achieve various characteristics such as viscosity, adhesion, mechanical strength, chemical resistance, and temperature resistance.

This study used a semi-transparent RTV-2 silicone with a hardness of 5 Shore, branded as VRM. The manufacturer recommended adding the silicone catalyst to a plastic container at a weight ratio of 2%. After ensuring that the mixture was thoroughly homogeneous, approximately 10 grams was poured onto the sandpaper as shown in Figure 2. Ultra-fine sandpaper with three different grit sizes was used, namely P800, P1200, and P2500. After curing at room temperature for 48 hours, the cured silicone film was peeled off from the paper, cut into 10 x 10 mm dimensions, and then placed into the TENG device for testing.

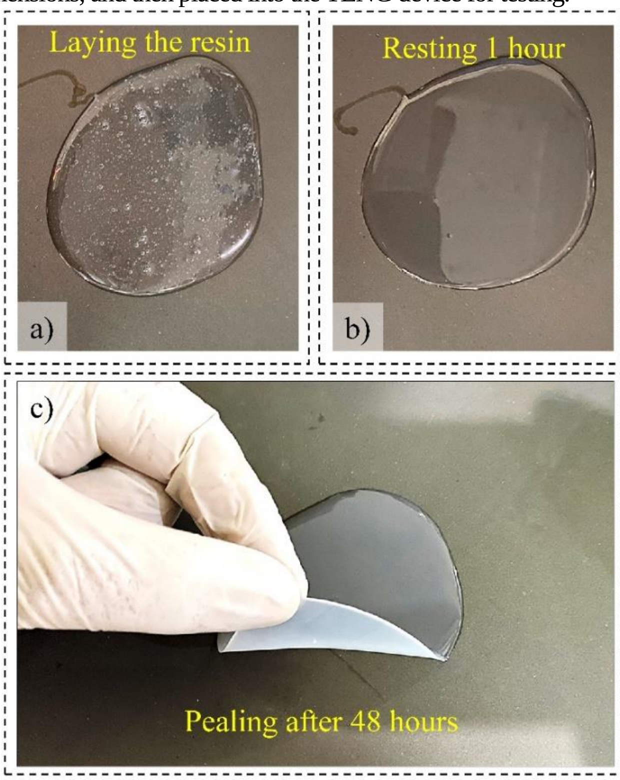

Fig. 2. Preparation of samples made of RTV2 silicone, (a) laying the mixture on sandpaper, (b) letting the air bubbles come out after 1 hour of rest, and (c) stripping the sample after two days.

2.3. Experimental Setup:

Figure 3 illustrates the setup used to measure the triboelectric performance of the samples. In this setup, a TENG was subjected to a uniform harmonic motion using a step motor programmed with Arduino Uno, ensuring the reproducibility of the experiments. The step motor was also controlled with an Arduino Uno board. The force applied to the setup (7.5 Newton) and pressure (75 kPa) was kept constant for each sample via a load cell. This load was monitored through the Arduino Uno board using the serial port on the computer screen. A Uni-T brand oscilloscope was utilized to monitor and record the generated voltage values.

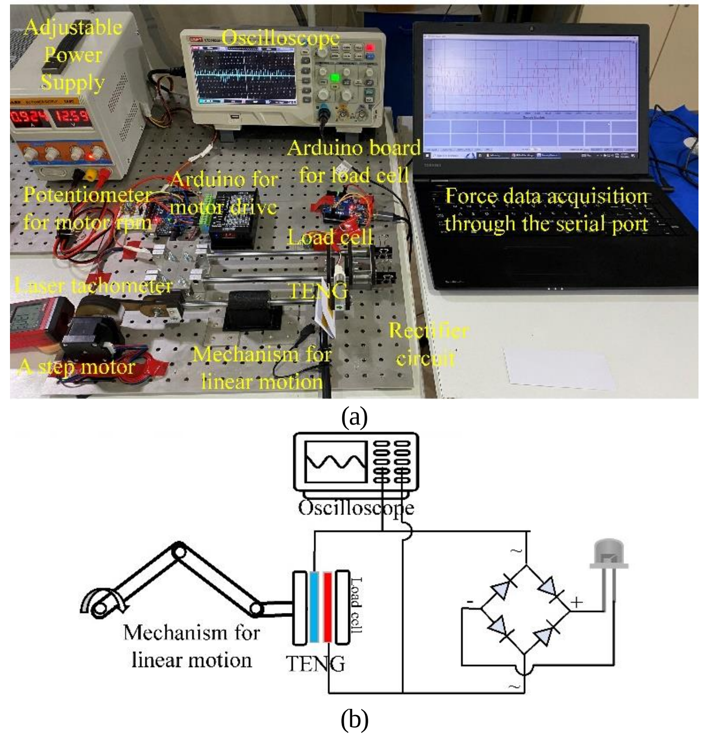

Fig. 3. (a) Components of experimental setup and (b) single-line diagram of the setup.

2.4. Sample Types

TENG pairs were produced after preparing the materials, as shown in Table 1. Four samples, *S0, S1, S2,* and *S3,* were designed and fabricated. The surfaces of these samples were examined for surface morphology using an optical microscope before the TENG measurements.

Table 1. Sample types and their pairs.

Sample name	*Inner tube*	*RTV2*
S0	No sanding cleaned the inner surface of the tube	The upper surface of the film has no grit pattern
S1	Sanded with P800	Patterned with P800
S2	Sanded with P1200	Patterned with P1200
S3	Sanded with P2500	Patterned with P2500

Finally, a larger sample (33 mm x 33 mm) was produced to replicate the dynamics closer to real-world conditions, selected from the sample type that showed the best performance. Voltage generation and LED lighting performance were investigated and reported.

3. RESULTS AND DISCUSSION

Figure 4 displays microscope images of samples produced from the inner tube material with sanding applied. The white spots observed in Figure 4(a) and Figure 4(e) may likely result from Talc or another additive mixed into the material paste. As the grit size decreased during the sanding process (finer), it was observed that the white spots diminished. In Figure 4(b), fibrillations can be seen, which have reduced in finer sanding. Although decreased in Figure 4(c), these still visible fibrils have become nearly indistinct in Figure 4(d).

Using a finer grit when sanding can generally be expected to produce a finer surface finish. However, materials such as rubber are highly flexible and soft and can exhibit different dynamics. In this case, the coarser grit sandpaper (*P800*) unexpectedly produced a more fibrillated surface on sample S1 than the others. The surface appears cleaner and more uniform when comparing the *S3* sample in Figure 4(d) and *h* with the *S0* sample. Additionally, forming very fine striped patterns is an expected outcome from using super fine sandpaper-like *P2500*.

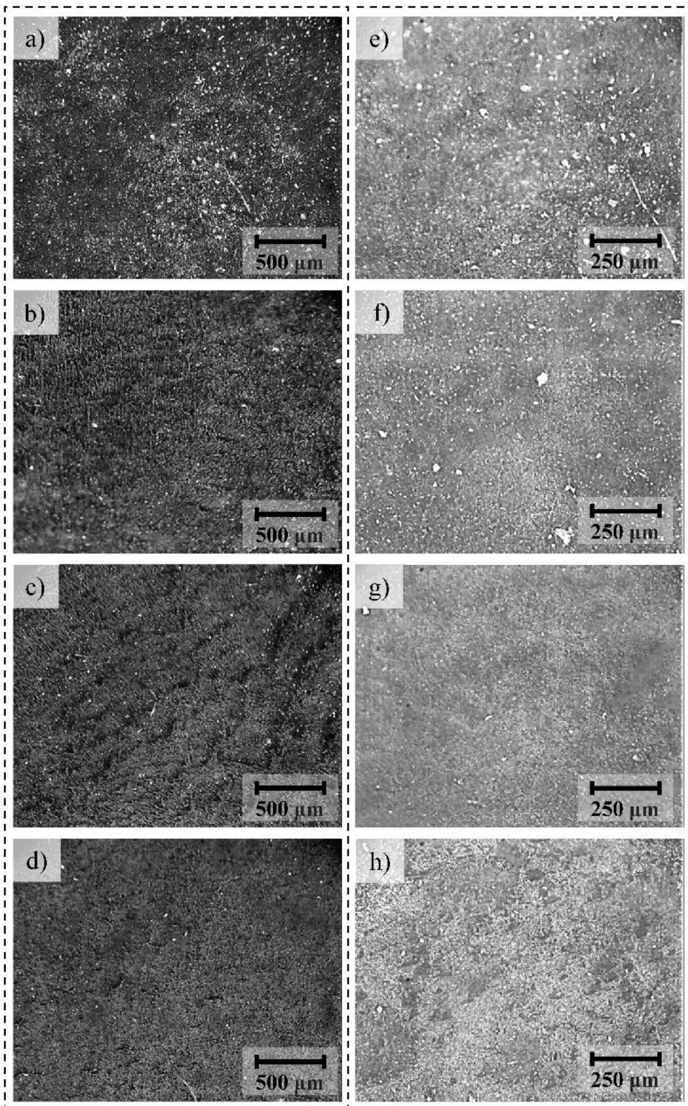

Fig. 4. Microscope images of inner tube samples are presented in a structured format. Each image on the right column is a higher magnification of its corresponding image on the left. The samples are labeled as follows: a) *S0*, b) *S1*, c) *S2*, and d) *S3*.

Figure 5 displays microscope images of RTV2 samples. Figures 5(a) and (b) show the presence of some trapped air bubbles, suggesting that additional treatments may be required to produce a completely bubble-free structure. The transition in pattern between the S1 sample in Figures 5(b) and Figures 5(f) and the *S2* sample in Figures 5(d) and Figures 5(g) is generally as expected, i.e. finer sandpaper produced a finer pattern on the RTV2. However, the large linear irregular structures in the pattern of the *S3* sample indicate a flaw coming from the sandpaper. Moreover, the absence of a clear fine pattern compared to *S2* could signify that some air bubbles remained in the RTV during its curing on the paper, possibly due to the fine grits not venting easily.

Figure 6 displays open-circuit voltage values and rectified graphs. Figure 6(a) and Figure 6(e) show the voltage values of the *S0* samples. The *S0* sample, which produced less than 2 V, had the worst performance compared to the others. Sample *S1* improved and produced an average voltage of about 4 V. Samples *S2* and *S3* showed similar performance. *S2* showed a slightly better performance with an average value just above 6 V, while the *S3* sample performed slightly below 6 V.

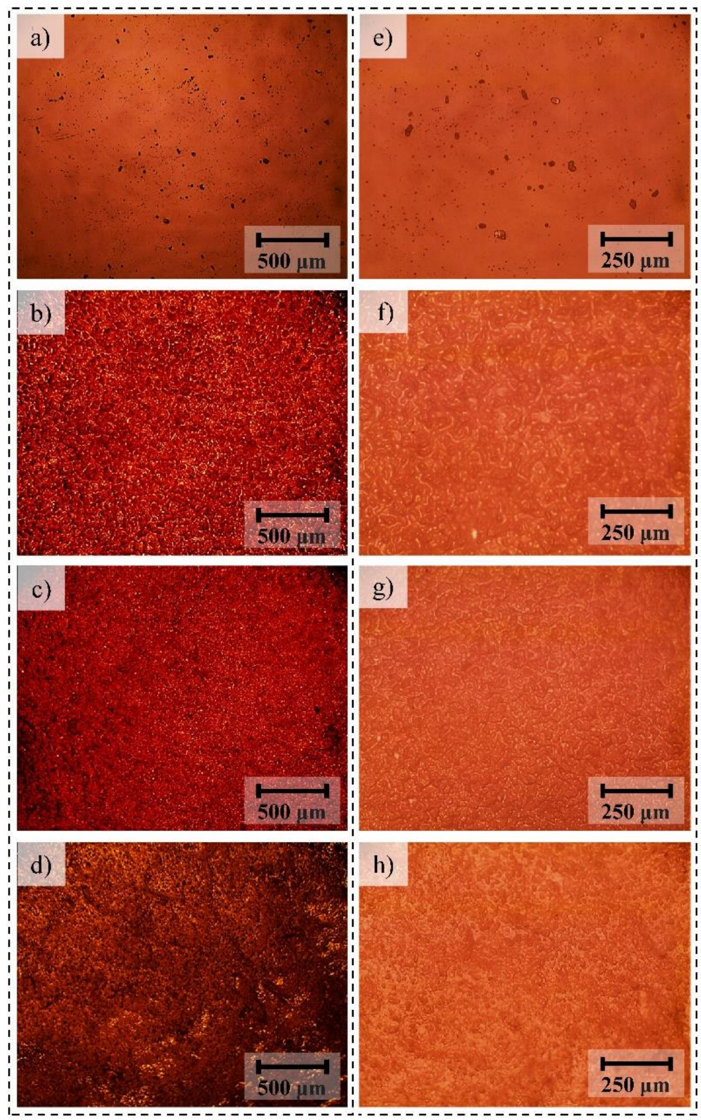

Fig. 5. Microscope images of RTV samples are presented in a structured format. Each image on the right column is a higher magnification of its corresponding image on the left. The samples are labeled as follows: a) *S0*, b) *S1*, c) *S2*, d) *S3*.

The presence of a relationship between the surface patterns of the samples and their voltage performance was demonstrated by the lower performance of the *S0* sample compared to the others. It can be inferred that having as rough and uniform a surface as possible is a crucial criterion for achieving the best performance. When examining the surface morphologies, it becomes evident that the *S2* sample was the top candidate, and the fact that its voltage value was better than the others supports the validity of this interpretation.

Overall, when looking at the rectified plots, it's clear that the negative side doesn't produce any significant voltage. Furthermore, the lack of a significant effect of the rectification process on the performance values contributes to the practical usability potential of these TENG samples.

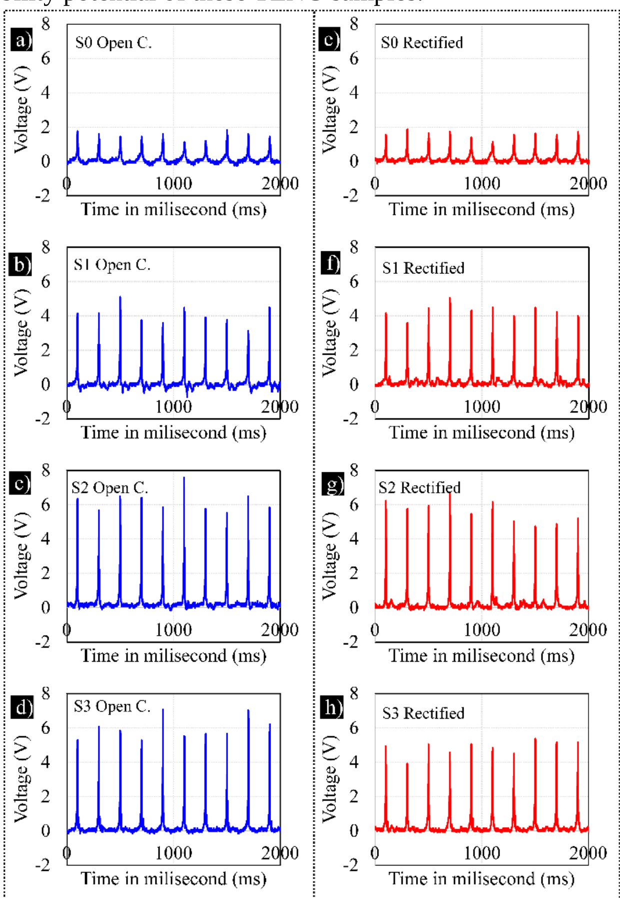

Fig. 6. Open circuit voltage values; the right column shows rectified graphics. a) *S0* open, b) *S1* open, c) *S2* open, d) *S3* open, e) *S0* rectified, f) *S1* rectified, g) *S2* rectified, and h) *S3* rectified.

Figure 7 shows the voltage values generated at various resistance values. When the resistance value was below 10 kΩ, all samples' energy and voltage generation potentials significantly decreased. While the *S2* and *S3* samples showed similar power generation potential, the S1 sample deviated negatively. As expected, the *S0* sample showed the worst performance. It was evident that using a resistance value greater than 1 million ohms can be beneficial in maximizing the energy potentials of the samples.

While the TENG measurement setup enhances the repeatability and comparability of experiments, practical applications often involve much more dynamic conditions. Therefore, a larger *S2* sample, which exhibited the best performance under more realistic conditions, was produced with an area of (33x33 mm²) and subjected to testing using a sports shoe. This sample and the test results are presented in Figure 8. The results clearly shows that the *S2* sample could generate significantly higher voltage when subjected to the realistic conditons. Its potential to generate 15 V and above was evident. Additionally, it successfully illuminated four LEDs with ample power. Therefore, it has a more significant energy generation potential under real-world conditions.

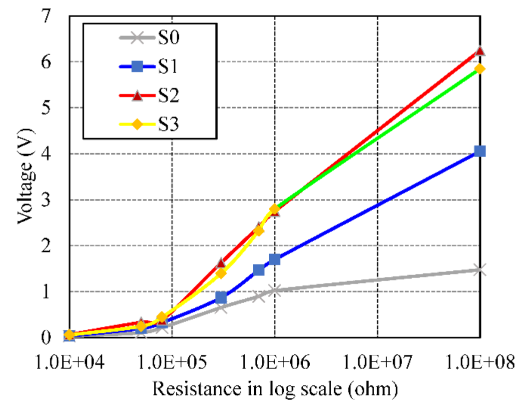

Fig. 7. Peak voltage values generated at various resistance.

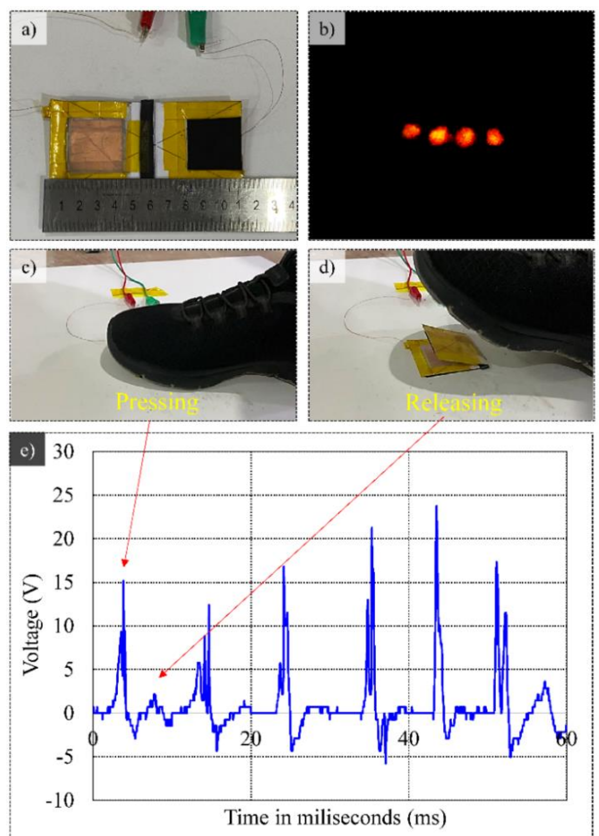

Fig. 8. Testing of the S2 TENG sample under realistic conditions, (a) An image of the TENG device, (b) An image of the moment when 4 LEDs are lit, (c) The moment of shoe compression, (d) The moment of shoe release, and e) the generated voltage values.

5. CONCLUSIONS

This study has successfully used upcycling methods to reprocess used inner tube rubber into an energy-harvesting device. The summary and findings of the study are presented in bullet points below:

- Scrap inner tube rubber has been processed using a suitable mass production method to improve the Triboelectric Nano Generator's (TENG) performance.
- The surface pattern of the rubber was modified using three different levels of sandpaper: *P800* (21.8 µm), *P1200* (15.3 µm), and *P2500* (8 µm) grit sizes, resulting in a total of four samples, including one without sanding.
- Small distinct fibrils were observed on the surface processed with P800 sandpaper, but their quantity decreased as finer sandpaper was used.
- The RTV material was selected as the electron acceptor, and films were created by mimicking the surface pattern of the sandpaper. Although some uneven characteristics were detected on the surface generated by *P2500* sandpaper.
- Among all samples, the *S2* sample exhibited the best performance, producing peak voltages comfortably exceeding 6 volts in open circuit and rectified configurations.
- Tests conducted with various resistances showed no significant decrease in the ability of all samples to produce energy and voltage, provided that the average peak voltage values remained below 10 kΩ.
- In an experiment mimicking real-world test conditions, the S2 sample was tested with a sports shoe and easily generated a voltage exceeding 15 V, capable of lighting up four LEDs.

This study has shown the potential of scrap inner tube rubber as an efficient material for the triboelectric nanogenerator (TENG). Future research should focus on elucidating the dynamics of surface pattern formation in more detail and conducting material analyses of inner tubes obtained from different brands and products, considering their performance in TENG applications. The implications of this study on future TENG technologies involve investigating non-traditional materials, gaining a more comprehensive understanding of surface pattern dynamics, and performing thorough analyses of materials from various sources. These objectives enhance the fundamental comprehension of TENG technology and provide beneficial insights for developing more effective and adaptable energy harvesting devices.

Acknowledgement

I would like to express my gratitude to Emin Uslu for his valuable assistance in processing data and generating figures. I am also indebted to Muhammet Emin Keskin for his support in preparing samples and utilizing microscopy, as well as to Zekiye Ekineken for her contributions in conducting the experiments. Lastly, I thank Murat Çolak for his help and support throughout this research.

References

[1] S. Chu, Y. Cui, and N. Liu, ‘The path towards sustainable energy,’ *Nature Materials*, 16(1), pp. 16-22, 2016.

[2] S. Chu and A. Majumdar, ‘Opportunities and challenges for a sustainable energy future,’ *Nature*, 488(7411), pp. 294-303, 2012.

[3] N. G. Park, M. Grätzel, T. Miyasaka, K. Zhu, and K. Emery, ‘Towards stable and commercially available perovskite solar cells,’ *Nature Energy*, 1(11), pp. 1-8, 2016.

[4] M. E. Karahallı, H. Asav, T. Özden, and B. Arıkan, ‘Layout optimization for shingled solar cells,’ *Turkish Journal of Electromechanics and Energy*, 7(3), pp. 100–104, 2022.

[5] B. Gülmez, R. Köse, and O. O. Yolcan, ‘Important parameters in solar power plant installation and Analytical Hierarchy Process,’ *Turkish Journal of Electromechanics and Energy*, 6(1), pp. 18–24, 2021.

[6] D. A. King, ‘Climate Change Science: Adapt, Mitigate, or Ignore?,’ *Science*, 303(5655), pp. 176-177, 2004.

[7] T. Ackermann and L. Söder, ‘Wind energy technology and current status: a review,’ *Renewable and Sustainable Energy Reviews*, 4(4), pp. 315-374, 2000.

[8] Y. M. Wei *et al.*, ‘Self-preservation strategy for approaching global warming targets in the post-Paris Agreement era,’ *Nat Commun*, 11(1), pp. 1624-1625, 2020.

[9] C. Le Quéré *et al.*, ‘Fossil CO_2 emissions in the post-COVID-19 era,’ *Nat Clim Chang*, 11(3), pp.197-199, 2021.

[10] W. Xu *et al.*, ‘A droplet-based electricity generator with high instantaneous power density’, *Nature*, vol. 578(7795), pp. 302-396, 2020.

[11] H. Wu, N. Mendel, D. Van Den Ende, G. Zhou, and F. Mugele, ‘Energy Harvesting from Drops Impacting onto Charged Surfaces,’ *Phys Rev Lett*, 125(7), pp.078301, 2020.

[12] A. Chortos and Z. Bao, ‘Skin-inspired electronic devices,’ *Materials Today*, 17(7), pp.321-331, 2014.

[13] Y. Yang *et al.*, ‘Triboelectric nanogenerator for harvesting wind energy and as self-powered wind vector sensor system,’ *ACS Nano*, 7(10), pp. 9461-9468, 2013.

[14] L. Chen *et al.*, ‘Stretchable negative Poisson’s ratio yarn for triboelectric nanogenerator for environmental energy harvesting and self-powered sensor,’ *Energy Environ Sci*, 14(2), pp. 955-964, 2021.

[15] Z. Lin *et al.*, ‘Triboelectric Nanogenerator Enabled Body Sensor Network for Self-Powered Human Heart-Rate Monitoring,’ *ACS Nano*, 11(9), pp.8830-8837, 2017.

[16] H. Wu and Y. Cui, ‘Designing nanostructured Si anodes for high energy lithium-ion batteries,’ *Nano Today*, 7(5), pp. 414-429, 2012.

[17] J. Lee, A. Urban, X. Li, D. Su, G. Hautier, and G. Ceder, ‘Unlocking the potential of cation-disordered oxides for rechargeable lithium batteries,’ *Science (1979)*, 343(6170), pp. 519-522, 2014.

[18] T. B. Maden and M. E. Şahin, ‘Modeling of The PEM Type Fuel Cells,’ *Turkish Journal of Materials*, 4(1), pp. 1–10, 2019.

[19] M. E. Şahin, F. Blaabjerg, and A. Sangwongwanich, ‘A review on supercapacitor materials and developments’, *Turkish Journal of Materials*, 5(2), pp. 10-24, 2020.

[20] Y. Ziat, A. Benyounes, O. El Rhazouani, C. Laghlimi, and M. Hammi, ‘Single-walled carbon nanotubes for enhanced

performance of Li-ion batteries,' *Turkish Journal of Materials*, 3(2), pp. 61–64, 2018.
[21] N. A. Iqteit, M. Attoun, and M. A. Sninah, 'The future of the Hebron electrical grid with growing demand for electric cars,' *Turkish Journal of Electromechanics and Energy*, 7(1), pp. 15–21, 2022.
[22] H. Ryu *et al.*, 'High-Performance triboelectric nanogenerators based on solid polymer electrolytes with asymmetric pairing of ions,' *Adv. Energy Mater.*, 7(17), pp. 1700289, 2017.
[23] J. Wu, X. Wang, H. Li, F. Wang, W. Yang, and Y. Hu, 'Insights into the mechanism of metal-polymer contact electrification for triboelectric nanogenerator via first-principles investigations,' *Nano Energy*, vol. 48, pp. 607-616, 2018.
[24] J. W. Lee and W. Hwang, 'Theoretical study of micro/nano roughness effect on water-solid triboelectrification with experimental approach', *Nano Energy*, vol. 52, pp.315-322, 2018.
[25] S. Niu and Z. L. Wang, 'Theoretical systems of triboelectric nanogenerators', *Nano Energy*, vol. 14, 2014.
[26] S. Lee, Y. K. Park, and J. Lee, 'Upcycling of plastic and tire waste toward use as a modifier for asphalt binder,' *Energy and Environment*. pp. 09583x-23117x, 2023.
[27] X. Zhao, B. Boruah, K. F. Chin, M. Đokić, J. M. Modak, and H. Sen Soo, 'Upcycling to sustainably reuse plastics,' *Advanced Materials*, 34(25), pp. 2100843, 2022.
[28] L. S. T. J. Korley, T. H. Epps, B. A. Helms, and A. J. Ryan, 'Toward polymer upcycling-adding value and tackling circularity,' *Science*, 373(6550), pp. 66-69, 2021.
[29] C. Jehanno *et al.*, 'Critical advances and future opportunities in upcycling commodity polymers,' *Nature*, 603(7903), pp. 803-814, 2022.
[30] G. Genc and N. Akkus, 'Application oriented recycling and machinability of waste bio-composite materials,' *Turkish Journal of Materials*, 3(2), pp. 58–60, 2018.
[31] S. Zheng, M. Liao, Y. Chen, and M. A. Brook, 'Dissolving used rubber tires,' *Green Chemistry*, 22(1), pp. 94-102, 2020.
[32] K. Formela and J. T. Haponiuk, 'Curing characteristics, mechanical properties and morphology of butyl rubber filled with ground tire rubber (GTR),' *Iranian Polymer Journal*, 23(3), pp. 185-194, 2014.
[33] H. Bian *et al.*, 'High thermal conductivity graphene oxide/carbon nanotubes/butyl rubber composites prepared by a dry ice expansion pre-dispersion flocculation method,' *J Appl Polym Sci*, 139(14), pp. 51987, 2022.
[34] S. R. Scagliusi, E. C. L. Cardoso, and A. B. Lugão, 'Effect of gamma radiation on the mechanical and degradation properties,' in *TMS 2015 144th Annual Meeting & Exhibition*, pp. 1309-1316, Florida, 2015.

Biography

Galip Yılmaz received his B.Sc. degree in Mechanical Engineering from Manisa Celal Bayar University in 2010, and his M.Sc. and PhD degrees from the University of Wisconsin-Madison in 2014, and 2019, both in Mechanical Engineering. He is currently working as an assistant professor in the Department of Electronics and Automation at Bayburt University, Türkiye. His research interest includes materials science, polymer analysis, and their processing.
E-mail: galipyilmaz@bayburt.edu.tr